Journal of Solid State Chemistry **160,** 401–408 (2001)
doi:10.1006/jssc.2001.9254, available online at http://www.idealibrary.com on IDEAL®

X-Ray and TEM Studies of $CdTeMoO_6$ and $CoTeMoO_6$: A New Superstructure of Fluorite Type with Cation and Anion Deficiencies ($\blacksquare CoTeMo)(\square_2O_6$)

Y. Laligant[1]

Laboratoire des Fluorures, CNRS UMR 6010, Faculté des Sciences, Université du Maine, Avenue O. Messiaen, 72085 Le Mans Cedex 9, France

Received February 9, 2001; in revised form May 10, 2001; accepted May 25, 2001

The crystal structures of two telluromolybdates $CdTeMoO_6$ and $CoTeMoO_6$ have been solved *ab initio*. $CdTeMoO_6$ crystallizes in a tetragonal cell (space group No. 113, $P\bar{4}2_1m$, $Z = 2$) with $a = 5.2840(1)$ Å, $c = 9.0595(2)$ Å whereas $CoTeMoO_6$ crystallizes in orthorhombic space group $P2_12_12$ (No. 18) with two formula units in the unit cell of dimensions $a = 5.2545(1)$ Å, $b = 5.0653(1)$ Å, and $c = 8.8589(2)$ Å. The X-ray powder diffraction pattern data were refined by the Rietveld profile technique and led respectively to $R_{Bragg} = 0.07$ for $CdTeMoO_6$ and $R_{Bragg} = 0.07$ for $CoTeMoO_6$. The crystal structure of $CdTeMoO_6$ is built up from corner-sharing distorted CdO_4 tetrahedra which build a layer in the a,b plane, while in $CoTeMoO_6$ cobalt atoms exhibited an octahedral distorted surrounding. Both compounds are simultaneously cation- and anion-deficient 1.1.2 superstructures of fluorite in which the electron lone pairs of tellurium are stereo-chemically active. High-resolution electron microscopy images of $CdTeMoO_6$ showed well-ordered crystals fragments, but in some crystals defects have also been detected. © 2001 Academic Press

Key Words: **oxides; *ab initio* structural determination; electron microscopy; X-ray diffraction.**

INTRODUCTION

Many works have been devoted to metal telluromolybdate $MTeMoO_6$ (M^{2+} = Cd, Co, Mn, Zn, Mg) (1–6) due to their catalytic properties for allylic oxidation of olefins. The corresponding X-ray diffraction patterns were tentatively indexed in an orthorhombic cell (space group $P2_12_12$, No. 18) with parameters listed in Table 1, except for $CdTeMoO_6$ which was also proposed to be tetragonal (space group $P4/n$ or $P4/nmm$) (5). Unfortunately until now accurate structural data were missing.

In an investigation aiming at clarifying the crystal structure of these phases, a study of the two compounds $CdTeMoO_6$ and $CoTeMoO_6$ was undertaken. These materials have been examined by X-ray powder diffraction, electron diffraction (ED), and high-resolution electron microscopy (HREM). The results were presented below.

[1]Fax: (33) 2 43 83 35 06. E-mail: yvon.laligant@univ-lemans.fr.

EXPERIMENTAL

The oxides $CdTeMoO_6$ and $CoTeMoO_6$ were prepared from a mixture of TeO_2 and $CdMoO_4$ or $CoMoO_4$ in the ratio 1:1 which were mixed in an agate mortar. The mixtures were placed in an alumina crucible and heated progressively to 600°C for 20 h and then slowly cooled to room temperature. The final products are respectively pale yellow for the cadmium compound and purple for the cobalt compound.

The powder X-ray patterns of these compounds were registered with a Siemens D501 diffractometer; the details of the collection are presented in Tables 2 and 3.

Thin specimens for electron microscopy were obtained by crushing and mounting the crystal fragments on a Cu grid covered with a carbon-coated holey film. Electron microscopy was performed with a JEOL-2010 electron microscope operating at 200 kV fitted with a side-entry $\pm 30°$ double-tilt specimen holder and equipped with a KEVEX energy-dispersive X-ray (EDX) analyzer.

The series of programs written by P. A. Stadelman (7) were used to simulate high-resolution images at different focus using the multislice method ($Cs = 1.0$ mm and $\Delta = 12$ nm) for different thicknesses of the crystals.

X-RAY AND ELECTRON DIFFRACTION

The cation composition was proven by EDX analyses ($CdTeMoO_6$, Cd:Te:Mo = 1:1:1; $CoTeMoO_6$, Co:Te:Mo = 1:1:1) calculated as a mean of 25 spot analyses.

Concerning the X-ray powder patterns, the reflection positions were estimated by means of the program EVA after stripping $K\alpha 2$. Autoindexing was performed by using

0022-4596/01 $35.00

TABLE 1
Crystal Data for $MTeMoO_6$ Telluromolybdates [from Ref. (3), Except * from Ref. (5)]

Compound	a (Å)	b (Å)	c (Å)	Space group
$MgTeMoO_6$	5.262	5.028	8.880	$P2_12_12$
$CoTeMoO_6$	5.262	5.062	8.857	$P2_12_12$
$ZnTeMoO_6$	5.255	5.044	8.909	$P2_12_12$
$MnTeMoO_6$	5.294	5.139	8.960	$P2_12_12$
$CdTeMoO_6$	5.279		9.056	$P4/n$ or $P4/nmm$
	5.53	5.10	9.08	* $P2_12_12$

TABLE 2
Conditions of X-Ray Data Collection and Crystallographic Characteristics of $CdTeMoO_6$

Diffractormeter	Siemens D501
Radiation	Cu$K\alpha$, graphite-diffracted beam monochromator 38 kV, 28 mA
Receiving slit (′)	0.05
Angular range (′2θ)	8–128 acquisition, 18–128 for refinement
Step scan increment (′2θ)	0.02
Count time (sec/step)	9
Miscellaneous	Room temperature, no sample rotation
Space group	$P\bar{4}\,2_1m$ (No. 113)
Cell parameters (Å)	$a = 5.2840(1)$, $c = 9.0595(2)$
Volume/Z	252.95 Å^3/$Z = 2$
Number of reflections	161
Number of refined parameters	25
Half-width parameters	$U = 0.048(2)$, $V = -0.025(2)$, $W = 0.0155(6)$
Peak shape, η	Pseudo-Voigt, 0.593(8)
Zero point (°2θ)	−0.1111(8)
Asymmetry parameters	$P1 = 0.078(9)$, $P2 = 0.064(2)$
Preferred orientation	[001] direction, 0.750(2)
Reliability factors with and without structure constraint[a]	$R_p = 0.12$, $R_{wp} = 0.16$, $R_{Bragg} = 0.07$, $R_F = 0.05$, $R_p = 0.09$, $R_{wp} = 0.13$

[a] R_p and R_{wp} are conventional Rietveld values, calculated after background subtraction.

the program TREOR (8) applied to the first 27 detected lines for $CdTeMoO_6$. Only one tetragonal solution was found and characterized by the conventional figures of merit $M_{27} = 99$ and $F_{27} = 130$ (0.00636) (9, 10). The condition-limiting reflections $hk0{:}h + k = 2n$ corresponded to the possible space groups $P4/nmm$ (No. 129) or $P4/n$ (No. 85). TREOR applied for $CoTeMoO_6$ led to only one orthorhombic solution with $M_{21} = 92$ and $F_{21} = 114$ (0.00534), $P2_12_12$ space group. This sample was contaminated by small amounts of $CoMoO_4$. Its structure was known so that its contribution is calculated and does not add new refined parameters but a scale factor.

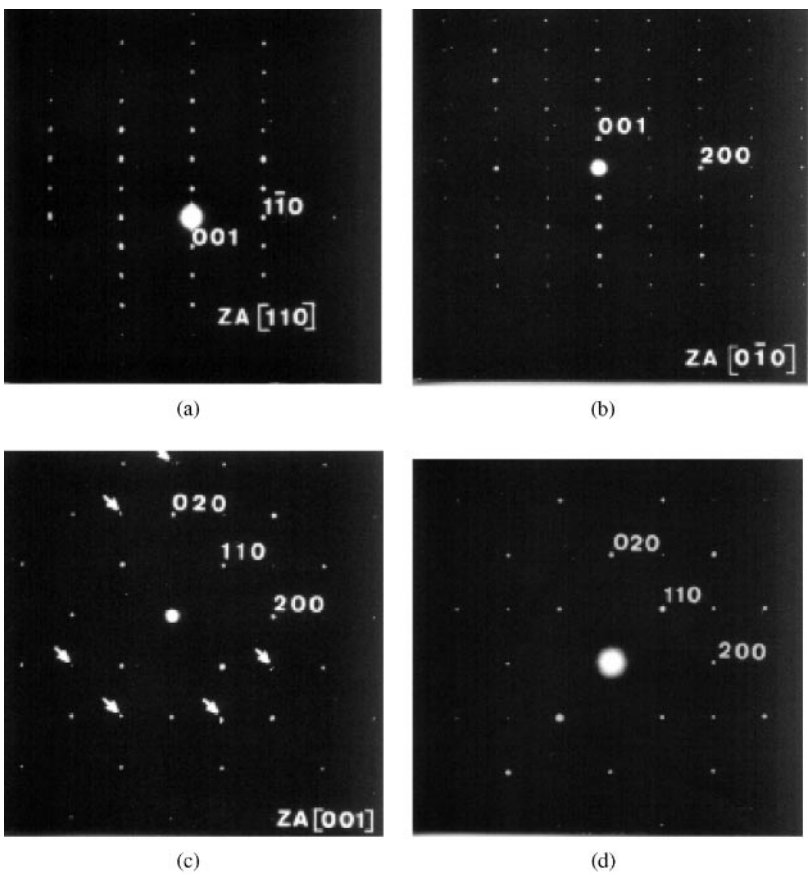

FIG. 1. ED patterns along [110] (a), [0$\bar{1}$0] (b) and [001] (c) zone axes from $CdTeMoO_6$. Small arrows indicate very weak reflections which violate the $hk0{:}h + k = 2n$ condition. For the sake of comparison, the [001] zone axis (d) of $CoTeMoO_6$ is also given.

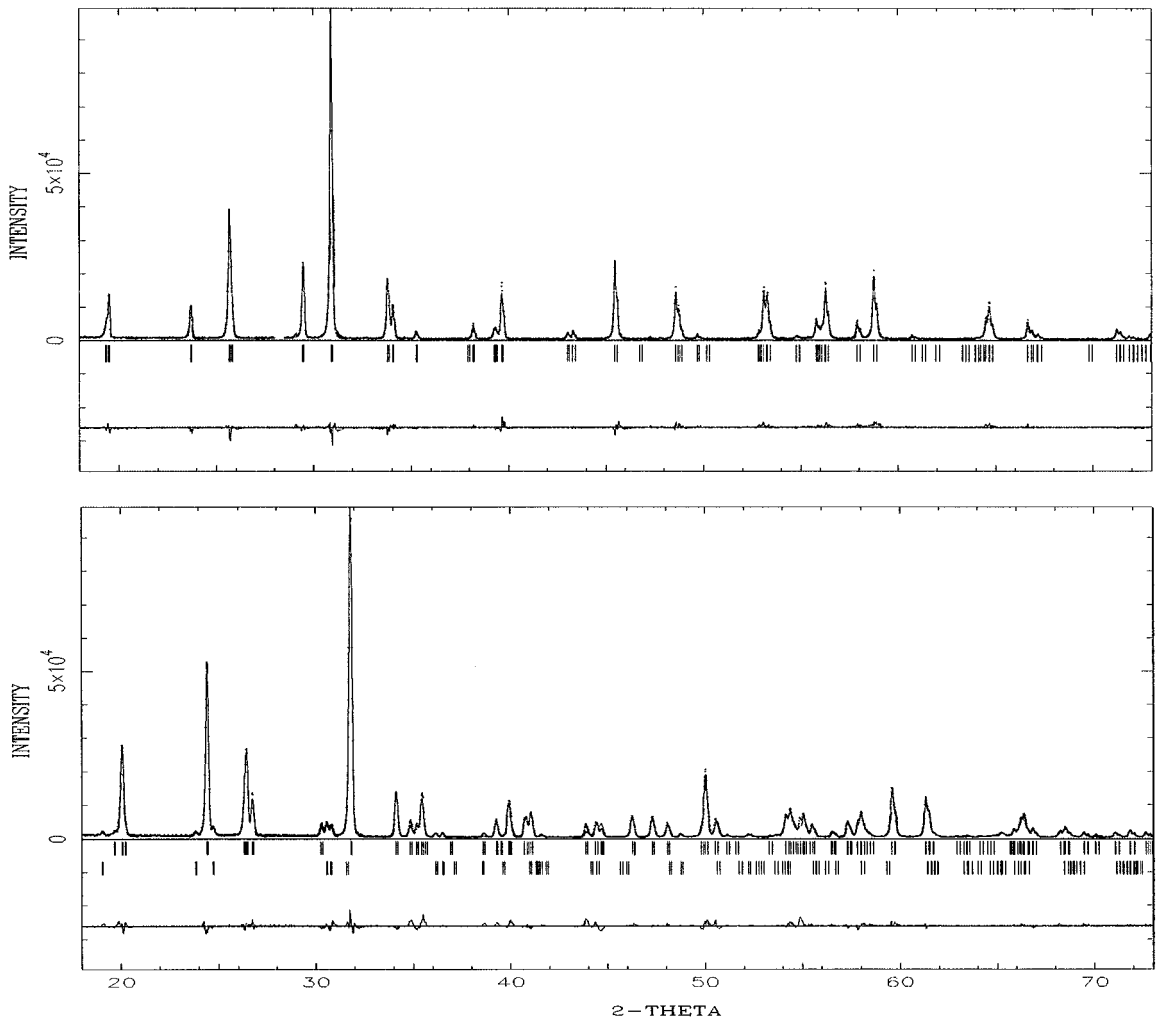

FIG. 2. (a) Final profile refinement of $CdTeMoO_6$. Observed (point), calculated (line), and difference (lower) profiles are shown. Vertical lines are reflection positions. (b) Final profile refinement of $CoTeMoO_6$. Observed (point), calculated (line), and difference (lower) profiles are shown. Vertical lines are reflection positions for $CoTeMoO_6$ (up) and $CoTeMoO_6$ (down).

Background correction was effected manually. In the 8–128° (2θ) angular range, a total of 220 "F_{obs}" amplitude factors were extracted by the Le Bail method (11), by iterating the Rietveld (12) decomposition formula in the less symmetrical space group $P4/n$. Calculations were performed by using the FULLPROF program (13).

Direct methods from the SHELXS-86 (14) program permitted location of the three heavy atom positions. Atomic

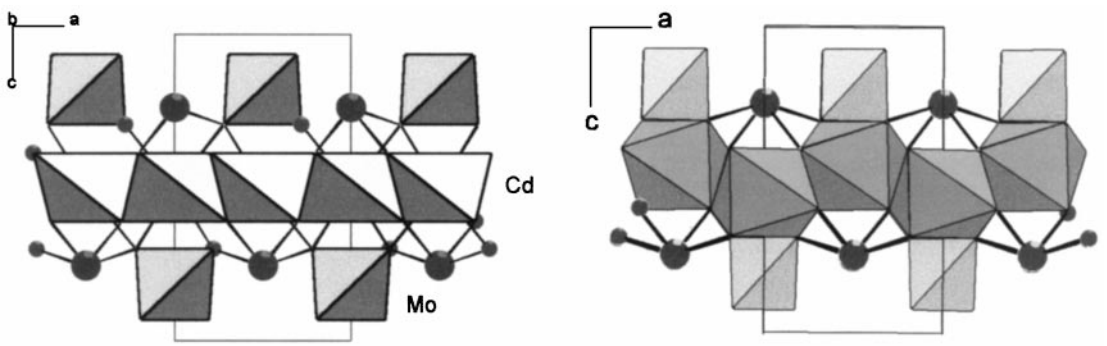

FIG. 3. (010) projections of the structure of $CdTeMoO_6$ (left) and $CoTeMoO_6$ (right).

TABLE 3
Conditions of X-Ray Data Collection and Crystallographic Characteristics of $CoTeMoO_6$

Diffractometer	Siemens D501
Radiation	Cu$K\alpha$, graphite-diffracted beam monochromator 38 kV, 28 mA
Receiving slit (′)	0.05
Angular range (′2θ)	8–128 for refinement
Step scan increment (′2θ)	0.02
Count time (sec/step)	9
Miscellaneous	Room temperature, no sample rotation
Space group	$P2_12_12$ (No. 18)
Cell parameters (Å)	$a = 5.2545(1)$, $b = 5.0653(1)$, $c = 8.8589(2)$
Volume/Z	235.78 Å^3/$Z = 2$
Number of reflections	257
Number of refined parameters	34
Half-width parameters	$U = 0.038(3)$, $V = -0.025(3)$, $W = 0.0268(9)$
Peak shape, η	Pseudo-Voigt, 0.393(9)
Zero point (°2θ)	0.0325(8)
Asymmetry parameters	$P1 = 0.161(7)$, $P2 = 0.044(2)$
Reliability factors with and without structure constraint[a]	$R_p = 0.12$, $R_{wp} = 0.16$, $R_{Bragg} = 0.07$, $R_F = 0.05$ $R_p = 0.08$, $R_{wp} = 0.12$
$CoMoO_4$	Pattern matching refinement
Number of refined parameters	1 (scale factor)

[a]See footnote *a*, Table 2.

TABLE 4
Atomic Coordinates and Thermal Parameters in Bold Characters for $CdTeMoO_6$ and in Italics for $CoTeMoO_6$[a]

Atom	Site	x	y	z	B_{iso} (Å^2)
Cd^{2+}	**2b**	**0**	**0**	**½**	**0.45(3)**
Co^{2+}	*2a*	*0*	*0*	*½*	*0.59(3)*
Te^{4+}	**2c**	**0**	**½**	**0.2421(1)**	**0.36(2)**
	2b	*0*	*½*	*0.2508(2)*	*0.26(3)*
Mo^{6+}	**2c**	**0**	**½**	**0.8148(2)**	**0.47(3)**
	2b	*0*	*½*	*0.8048(2)*	*0.41(4)*
O(1)	**4e**	**0.304(2)**	**0.804(2)**	**0.066(1)**	**1.2(2)**
	4c	*0.322(2)*	*0.826(2)*	*0.076(1)*	*0.9(2)*
O(2)	**4e**	**0.219(2)**	**0.719(2)**	**0.704(1)**	**0.9(2)**
	4c	*0.188(2)*	*0.762(3)*	*0.691(1)*	*0.8(2)*
O(3)	**4e**	**0.202(2)**	**0.702(2)**	**0.387(1)**	**1.4(2)**
	4c	*0.199(3)*	*0.696(2)*	*0.400(1)*	*1.3(2)*

[a]Standard deviations are given in parentheses.

scattering factors and anomalous dispersion terms were taken from the *International Tables for X-ray Crystallography* (15). Unfortunately, oxygen atoms could never be located on Fourier synthesis either in $P4/n$ or in $P4/nmm$.

The reconstruction of the reciprocal space of $CdTeMoO_6$ using electron diffraction allows a tetragonal cell to be evidenced with $a \approx 5.28$ Å and $c \approx 9.06$ Å. The condition-limiting reflections are $h00{:}h = 2n$, and $0k0{:}k = 2n$, compatible with the two space groups $P\bar{4}2_1m$ (No. 113) and $P42_12$ (No. 90). This is illustrated by the [110], [0$\bar{1}$0], and [001] ED patterns displayed in Fig. 1. The main difference with X-ray data was the loss of the condition $hk0{:}h + k = 2n$ which corresponded to weak peaks on electron diffraction patterns. The crystals exhibit a plate-like shape with the short dimension parallel to the c crystallographic axis.

At this stage, it is worth noting that a small orthorhombic distortion was observed on some diffraction patterns with $a \approx 5.26$ and $b \approx 5.30$ Å. In this particular case, the only space group deduced from systematic extinctions led to $P2_12_12$. Careful examination of the X-ray pattern did not indicate any splitting of the diffraction peaks.

By using the $P\bar{4}2_1m$ space group, the *ab initio* resolution by the SHELXS-86 program confirmed the cationic distribution found above. These positions formed the initial model for the RIETVELD refinements using the FULLPROF program. Three oxygen sites are located after subsequent cycles of refinement and difference Fourier synthesis with the program SHELXL-93 (16). Final Rietveld refinement (FULLPROF) for all atoms led to $R_{Bragg} = 0.07$. Table 2 gathers the crystallographic characteristics and the refined profile parameters together with the reliability factors for $CdTeMoO_6$. The same procedure for the structure

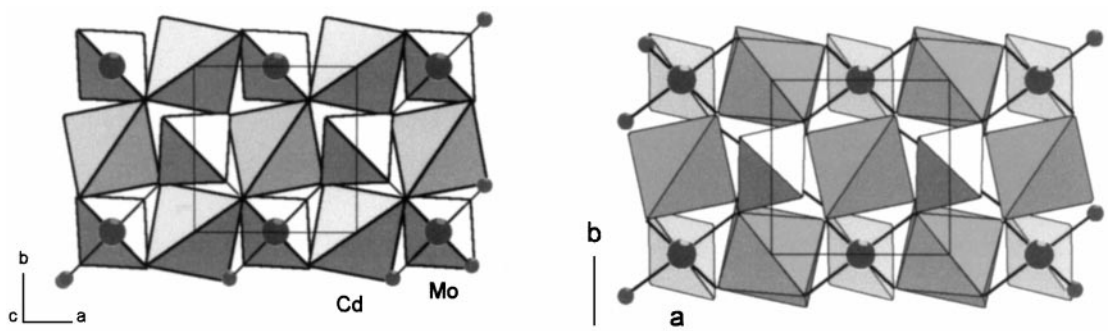

FIG. 4. (001) projections of the structure of $CdTeMoO_6$ (left) and $CoTeMoO_6$ (right).

TABLE 5
Selected Bond Distances (Å) and Bond Angles (°) for $CdTeMoO_6$ and in Italics for $CoTeMoO_6$[a]

Cd–O(3)	**4×2.159(10)**	**O(3)–Cd–O(3)**	**123.5(5)**
Cd…O(2)	**4×2.640(10)**	**O(3)–Cd–O(3)**	**102.9(2)**
$d_{Shannon}$ = 2.140	**⟨2.159⟩**		
Co–O(3)	*2 × 2.060(12)*	*O(3)–Co–O(3)*	*129.2(6)*
Co–O(3)	*2 × 2.066(13)*		*98.9(2)*
Co–O(2)	*2 × 2.301(12)*		*102.3(2)*
$d_{Shannon}$ = 2.105	*⟨2.142⟩*	*O(2)–Co–O(2)*	*85.3(6)*
		O(2)–Co–O(3)	*72.9(4)*
			157.7(4)
			67.0(4)
			76.2(4)
Te–O(3)	**2×2.002(9)**	**O(3)–Te–O(3)**	**97.9(5)**
Te–O(2)	**2×2.154(10)**	**O(2)–Te–O(2)**	**153.9(5)**
$d_{Shannon}$ = 2.020	**⟨2.078⟩**	**O(2)–Te–O(3)**	**81.5(4)**
Te–O(3)	*2 × 1.959(12)*	*O(3)–Te–O(3)*	*94.9(7)*
Te–O(2)	*2 × 2.101(12)*	*O(2)–Te–O(2)*	*151.6(6)*
$d_{Shannon}$ = 2.020	*⟨2.030⟩*	*O(2)–Te–O(3)*	*87.7(5)*
			73.1(5)
Mo–O(1)	**2×1.819(9)**	**O(1)–Mo–O(1)**	**107.0(6)**
Mo–O(2)	**2×1.920(10)**	**O(2)–Mo–O(2)**	**117.1(6)**
$d_{Shannon}$ = 1.770	**⟨1.870⟩**	**O(1)–Mo–O(2)**	**108.1(4)**
Mo–O(1)	*2 × 1.665(12)*	*O(1)–Mo–O(1)*	*101.0(8)*
Mo–O(2)	*2 × 1.935(12)*	*O(2)–Mo–O(2)*	*117.3(7)*
$d_{Shannon}$ = 1.770	*⟨1.800⟩*	*O(1)–Mo–O(2)*	*104.8(5)*
			114.0(5)

[a]Standard deviations are given in parentheses and average M–O distances in brackets.

determination of $CoTeMoO_6$ was applied leading to the results gathered in Table 3.

RESULTS AND DISCUSSION

The X-ray diffraction pattern plots are shown on Fig. 2. The atomic coordinates and thermal parameters are reported in Table 4. Selected interatomic distances and angles are listed in Table 5. The mean metal–oxygen distances are largely in agreement with the sum of ionic radii (17), but as usual for powder structure calculations one cannot expect a very high precision on the positional parameters of light atoms because of the presence of heavy scatterers.

Figure 3 shows the (010) projections of the structures of $CdTeMoO_6$ and $CoTeMoO_6$. The most striking feature concerns the coordination of the cations. All of them in the cadmium compound are four-fold coordinated, but in two different ways: tetrahedral for both Cd^{2+} and Mo^{6+}, bisphenoid for Te^{4+}.

The main difference between $CdTeMoO_6$ and $CoTeMoO_6$ lies in the coordination around Cd^{2+} and Co^{2+}: for Cd^{2+} as mentioned above four oxygens build up a tetrahedron CdO_4 (the next nearest neighbors found are $4 \times Cd–O2 = 2.640(10)$ Å) whereas six oxygens build up an

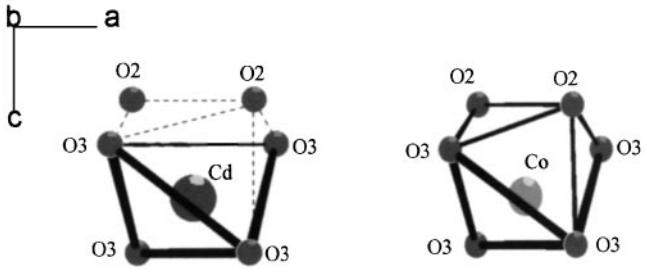

FIG. 5. Coordination around Cd^{2+} and Co^{2+}.

octahedron around Co^{2+} (Figs. 4 and 5). This was achieved by shifting the y coordinate of O(2). Such a distorted octahedral surrounding of Co^{2+} was found in the cobalt tellurite $Co_6(TeO_3)_4(TeO_4)$ (18).

The Te^{4+} coordination is typical of four-valent Te–O compounds featuring a distorted trigonal bipyramidal configuration around Te^{4+} with one of the equatorial positions left unoccupied (Fig. 6). Angles and distances within the TeO_4 unit are similar to those found for example in $Co_6(TeO_3)_4(TeO_4)$ (18) or in Refs. (19, 20).

Although there are some analogies between the crystal structure of $CdMoO_4$ and $CdTeMoO_6$ since both unit cells belong to the tetragonal system and have comparable a axis lengths, $CdMoO_4$ belongs to the scheelite type with space group $I4_1/a$ (21, 22). The different symmetry space groups require different arrangements of the structural units in the unit cells. Indeed the shape of $CdTeMoO_6$ crystals suggests a layer structure which does not occur in the scheelite-type structure of $CdMoO_4$. Moreover in $CdMoO_4$ the Mo^{6+} cation is tetrahedrally coordinated (4×1.823 Å) as in $CdTeMoO_6$ but Cd^{2+} was found height-fold coordinated (4×2.281 Å, 4×2.503 Å).

Cations constitute a slightly distorted ffc network ($a_F \approx 5.2$ Å) with distances between nearest neighbors ranging from 3.36 to 3.77 Å. Figures 7 and 8 show how the ordered formation of vacancies within the anionic and cationic subarray of the fluorite structure leads, after small shifts, to the $CoTeMoO_6$ superstructure. Anions (O2 and

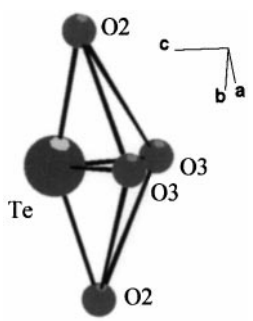

FIG. 6. Te^{4+} coordination polyhedron.

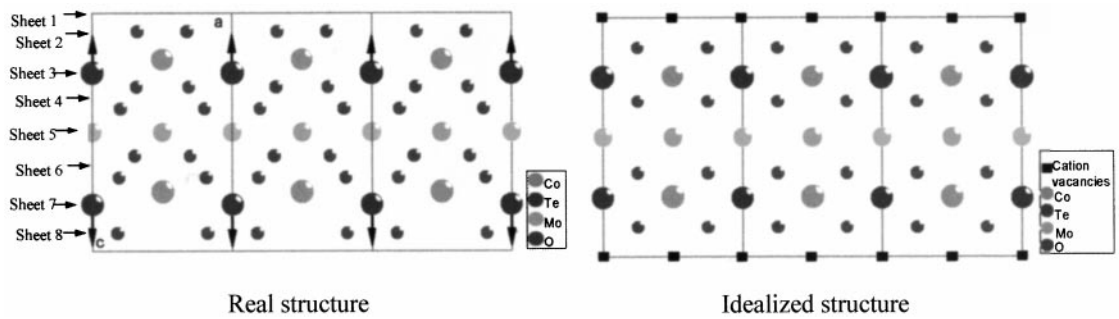

FIG. 7. Projection of the structure of $CoTeMoO_6$ onto the x, z plane showing how the sheets are stacked.

O3) approximately occupy all the tetrahedral sites of this structure (8/8—sheets 4 and 6 on Fig. 8) whereas O1 occupies, in an ordered way, only 4/8 sites (sheets 2 and 8 in Fig. 8). All the anions led to a total occupancy of 6/8. $CoTeMoO_6$ can therefore be considered as an anion-deficient fluorite-like 1.1.2 superstructure and can be written, $(Co_2Te_2Mo_2)(\square_4O_{12})$.

In fact, because of the disparity in size of the cations (Co^{2+} or Cd^{2+}, Te^{4+}, and Mo^{6+}) and of the stereochemical activity of the lone pair of the Te^{4+} cations (Fig. 7), nearly

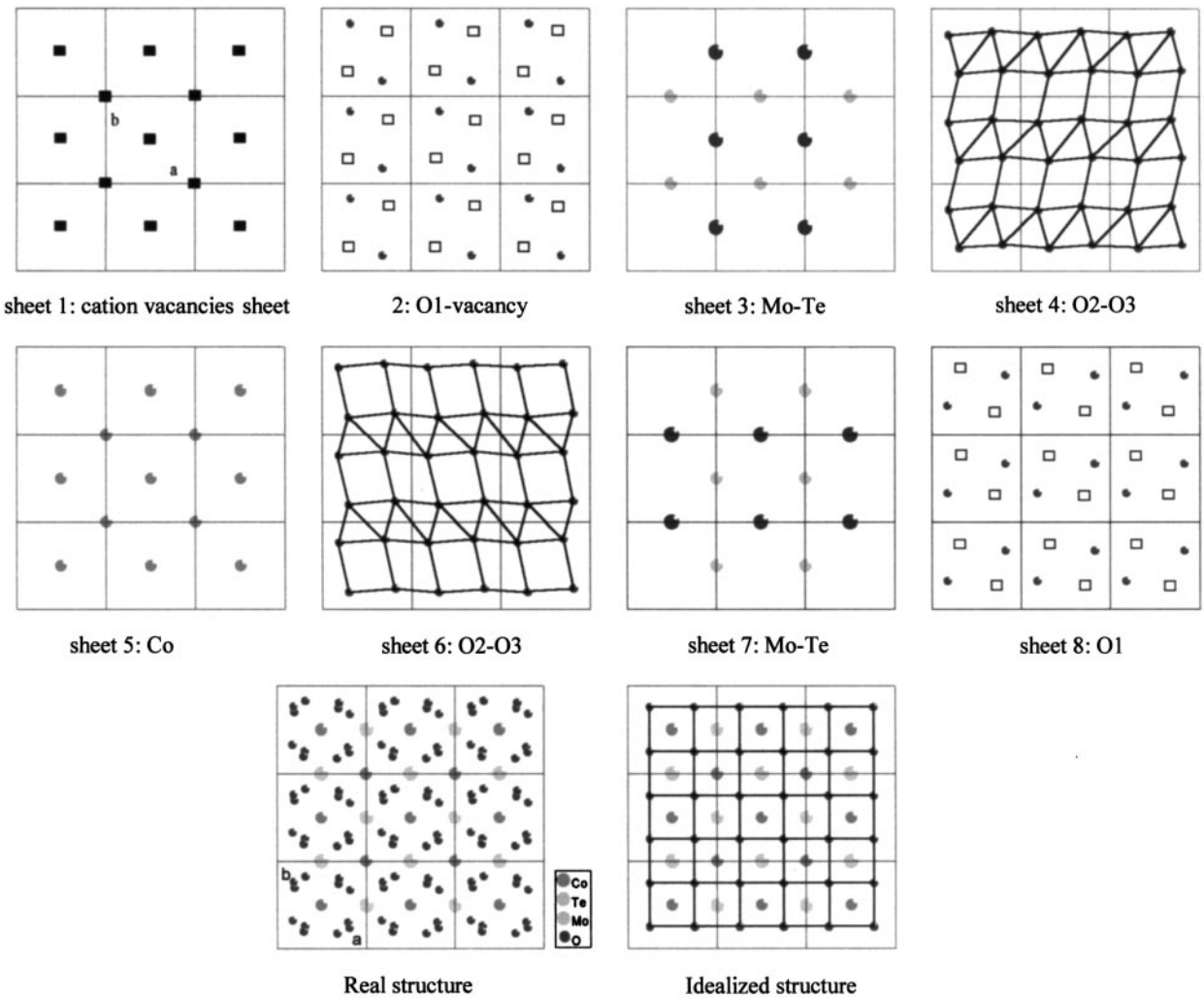

FIG. 8. Details of the layers within (001) sheets showing how the cation and anion deficiencies are accommodated.

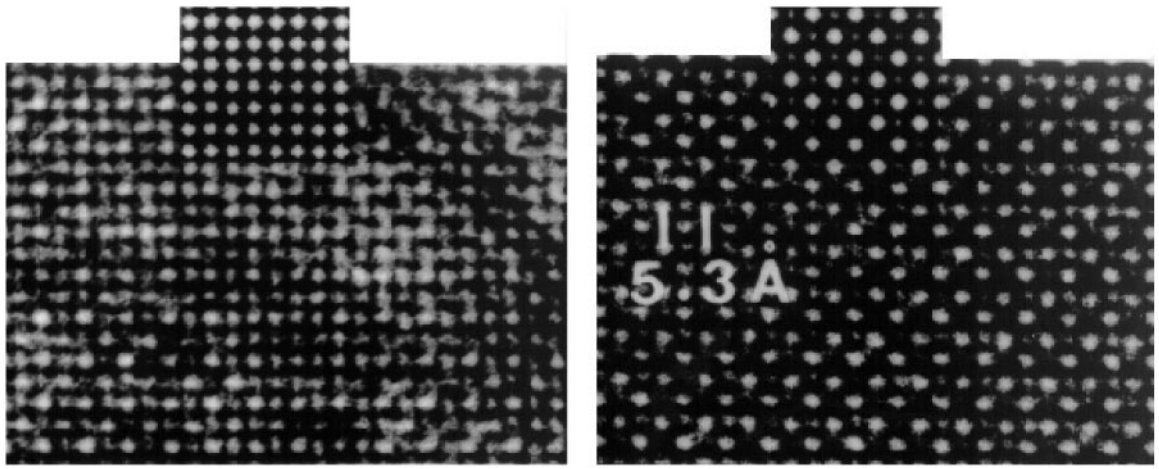

FIG. 9. Characteristic HREM experimental [001] images of $CdTeMoO_6$ with the calculated images in inset (thickness: 45 Å), defocus values: (a, left) −780 Å, (b, right) −500 Å.

all the anions are set off-center toward either one face or one edge of the tetrahedron, and so are essentially in three-fold coordination.

Furthermore, both compounds exhibit cation-deficient fluorite-type superstructure (sheet 1 in Fig. 7) leading to $(\blacksquare_2Co_2Te_2Mo_2)O_{12}$. By taking into account both cation and anion deficiency, the formula can be written as $(\blacksquare_2Co_2Te_2Mo_2)(\square_4O_{12})$ for one unit cell, or more simply:

$$(\blacksquare CoTeMo)(\square_2O_6) \rightarrow (\blacksquare M_3)(\square_2O_6) \rightarrow$$

$$(\blacksquare_{1/3}M)(\square_{2/3}O_2).$$

It is worth noting that cations and anions correspond exactly to the fluorite structure MO_2 together with the vacancies on cation and anion networks $\blacksquare\square_2$.

As indicated by the projections of Fig. 8, the reorganization mentioned above corresponds to the transformation of the square 4^4 anionic layers of the parent fluorite structure into $3^3 \cdot 4^2$ layers (sheets 4 and 6). This net is intermediate between 4^4 and 3^6 (23). Usually, shearing of a 4^4 net of anions to a 3^6 net of anions results in a higher packing density which enables the excess anions in the $Zr(N, O, F)_x$ system to be accommodated (24 and references therein).

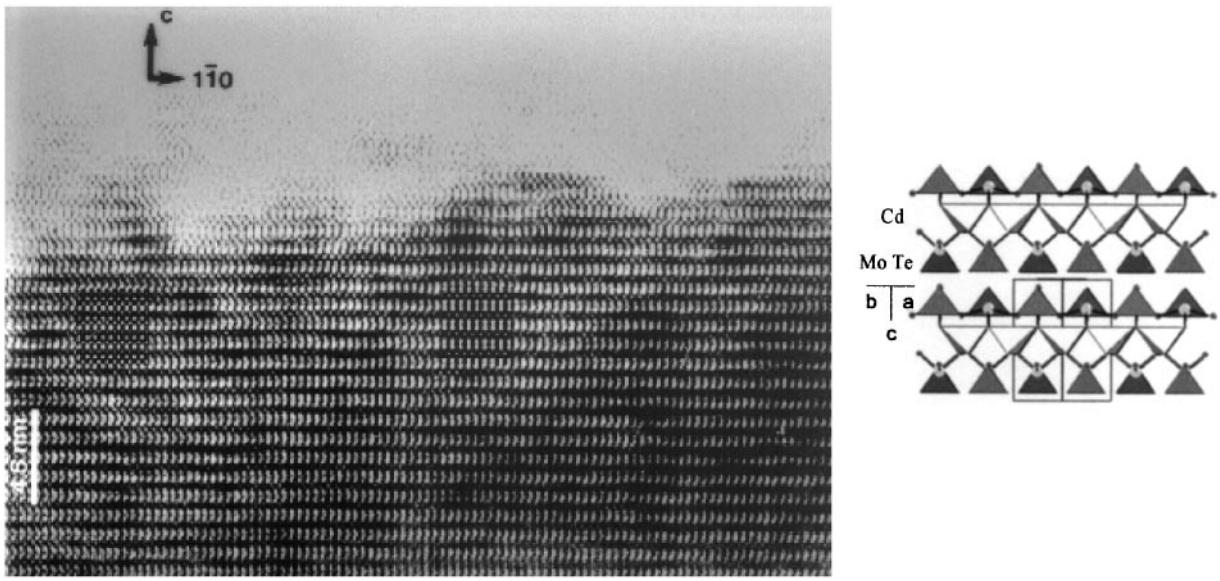

FIG. 10. High-resolution [110] image for a defocus value of −620 Å. A small variation of the crystal thickness induced very fast variation of the observed contrast: (left) thickness = 37 Å, (right) thickness = 22 Å. For comparison the [110] projection of the crystal structure is given.

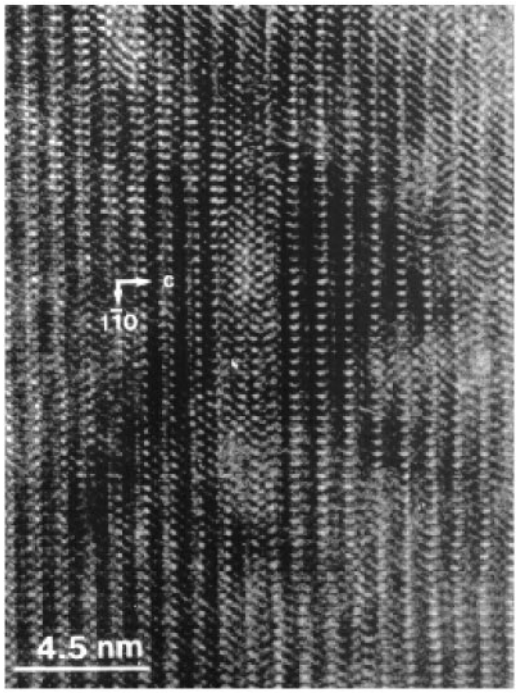

FIG. 11. Stacking faults as observed by HREM along the [110] direction.

HIGH-RESOLUTION ELECTRON MICROSCOPY

$CoTeMoO_6$ was found to be sensitive to the electron beam, resulting in a fast amorphization of the thinner edges of the crystal during high-resolution work and irradiation damage in the bulk.

$CdTeMoO_6$ was found to be more stable under electron beam and high-resolution work became possible. These observations can be correlated with the thermal behavior of both compounds: $T_f = 650$–$680^\circ C$ for $CoTeMoO_6$ (3, 5) and $760^\circ C$ for $CdTeMoO_6$ (3).

HREM-simulated images were calculated using the model determined by X-ray diffraction and were compared to the experimental images of $CdTeMoO_6$. Calculated through focus series along the [001] orientation fit well with the experimental images and allowed an interpretation of the observed contrasts to be given. Figure 9a corresponds to a defocus value of -780 Å close to Scherzer: white dots are representative of the lowest electronic densities, and all atoms appear in black. On the photograph of Fig. 9b which was obtained for a defocus value of -500 Å, the white intense dots correspond to Mo and Te atoms whereas Cd atoms appear in black.

An image recorded along the [110] zone axis is presented in Fig. 10. On the left part of this image all the cations appear as black dots and the low electronic density is white. On the right part of the same image, a different contrast in the Cd and Te–Mo planes can be clearly distinguished as a result of the ordering between both cations: the black ribbons with gray spots correspond to cadmium layers and the white sticks are representative of two successive Te–Mo layers.

Defects shown in Fig. 11 are stacking faults which correspond to an irregular arrangement of the Cd and Mo–Te layers.

REFERENCES

1. P. Forzatti and G. Tieghi, *J. Solid State Chem.* **25,** 387 (1978).
2. R. Kozlowski and J. Sloczynski, *J. Solid State Chem.* **18,** 51 (1976).
3. P. Forzatti and P. Tittarelli, *J. Solid State Chem.* **33,** 421 (1980).
4. G. Tieghi and P. Forzatti, *J. Appl. Crystallogr.* **11,** 291 (1978).
5. I. L. Botto and E. J. Baran, *Z. Anorg. Allg. Chem.* **468,** 221 (1980).
6. J. Sloczynski, *Z. Anorg. Allg. Chem.* **438,** 287 (1978).
7. P. A. Stadelman, *Ultramicroscopy* **21,** 131 (1997).
8. P. E. Werner, L. Eriksson, and M. Westdhal, *J. Appl. Crystallogr.* **18,** 367 (1985).
9. P. M. De Wolff, *J. Appl. Crystallogr.* **1,** 108 (1968).
10. G. S. Smith and R. L. Snyder, *J. Appl. Crystallogr.* **12,** 60 (1979).
11. A. Le Bail, *NIST Special Publ.* **846,** 213 (1992).
12. H. M. Rietveld, *J. Appl. Crystallogr.* **2,** 65 (1969).
13. J. Rodriguez-Carvajal, "Program FULLPROF," Version 3.5, 1998.
14. G. M. Sheldrick, "SHELXS-86, in Crystallographic Computing 3" (G. M. Sheldrick, C. Krüger, and R. Goddard, Eds.), Oxford Univ. Press, London, 1985.
15. "International Tables for X-ray Crystallography," Vol. C. Kluwer, Dordrecht, 1992.
16. G. M. Sheldrick, "SHELXL-93: A program for the refinement of crystal structures from diffraction data." University of Göttingen, Germany, 1993.
17. R. D. Shannon, *Acta Crystallogr. A* **32,** 751 (1976).
18. M. Trömel and Th. Scheller, *Z. Anorg. Allg. Chem.* **427,** 229 (1976).
19. K. Kohn, K. Inoue, O. Horie, and S. I. Akimoto, *J. Solid State Chem.* **18,** 27 (1976).
20. C. Olsson, L. G. Johansson, and S. Kazikowski, *Acta Crystallogr. C* **44,** 427 (1988).
21. A. V. Chichagov, L. N. Dem'yanets, V. V. Ilyukin, and N. V. Belov, *Kristallografiya* **11,** 686 (1966).
22. A. W. Sleight, *Acta Crystallogr. B* **28,** 2899 (1972).
23. M. O'Keeffe and B. G. Hyde, *Philos. Trans. R. Soc. London Ser. A* **295,** 553 (1980).
24. R. L. Withers, S. Schmid, and J. G. Thompson, *Prog. Solid Stare Chem.* **26**(1), 1 (1998).